Fe_3O_4 Nanoparticles, Metal–Organic Framework of Zr and Cu, and their Composites: Synthesis, Characterization, and Photocatalytic Activity

[1]Reazul Hasan Riyan, [1]Muhaimin Helal Efat, [1]Md. Azharul Arafath* and [2]Md. Sohrab Hossain
[1]Department of Chemistry, School of Physical Sciences, Shahjalal University of Science and Technology, Sylhet 3114, Bangladesh.
[2]HICoE-Centre for Biofuel and Biochemical Research, Institute of Self-Sustainable Building, Department of Fundamental and Applied Sciences, Faculty of Science and Information Technology. Universiti Teknologi PETRONAS, Seri Iskandar 32610, Perak Darul Ridzuan, Malaysia.
arafath-che@sust.edu*

(Received on 27th February 2025, accepted in revised form 22nd August 2025)

Summary: Fe_3O_4 nanoparticles (a), novel Fe_3O_4/Zr-MOF (b) and Fe_3O_4/Cu-MOF (c) composites with Zr and Cu metal-organic framework Zr-MOF (d) and Cu-MOF(e) were synthesized. Fe_3O_4 nanoparticles Zr-MOF (d) and Cu-MOF (e) were synthesized by hydrothermal method and Fe_3O_4/Zr-MOF and Fe_3O_4/Cu-MOF composite was synthesized by sonication. The photocatalytic activity of the Fe_3O_4 (NPs), MOFs and the composites were investigated for degradation of methylene blue exposed to sunlight at pH 9.2. The composites were characterized by FTIR, UV-vis, TGA, SEM, and EDS spectroscopy. The composites Fe_3O_4/Zr-MOF and Fe_3O_4/Cu-MOF showed the highest efficiency of 87% and 96% respectively, whereas nanoparticle Fe_3O_4 (NPs) exhibited efficiency of 77%. The of MOF, Zr-MOF and Cu-MOF individually showed less efficiency of 41%, and 49% respectively. The composite Fe_3O_4/Zr-MOF and Fe_3O_4/Cu-MOF showed 1.13 and 1.24-times higher efficiency respectively over Fe_3O_4 (NPs) and more than double of MOF. The incorporation of Fe_3O_4 NPs in the Zr-MOF and Cu- MOF tune the band gap to an optimal level for radical formation and sustain required time to initiate photochemical reaction. The band gap of Fe_3O_4 (NPs) and Fe_3O_4/Cu-MOF composite is 1.95 eV and 2.54 eV respectively, whereas the band gap for TiO_2 is approximately 3.2 eV which is established photo-catalyst. It is observed that Fe_3O_4/Cu-MOF (c) composites band gap closer to TiO_2 and shows higher efficiency. These composites showed outstanding degradation efficiency than current established photocatalyst. So, these could be used industrial pollution mitigation for green environment.

Keywords: Composite; Methylene Blue; MOF; Nano oxide; Photodegradation; and SEM.

Introduction

Globally, industrialization is drastically increasing, fresh water reservoirs are being contaminated on a regular basis. Organic residues, organic dyes from textile industries, and other industrial wastes are the major contributors to contaminate water resources and environment [1]. The presence of organic pollutants, particularly synthetic dyes, stimulates microbial growth in river. This causes the river ecosystem's degradation and disturbance of required oxygen level for aquatic life. Hence, purifying of the wastewater that discharged from industries has become a crucial concern. Methylene blue (MB) is widely recognized for its applications as a dye and in clinical interventions, notably for methemoglobinemia but its improper administration or over use can lead to various negative health impacts, including hypertension, headaches, hemolysis, dyspnea, serotonin syndrome, vomiting. MB can reduce hemoglobin iron from the Fe^{3+} (ferric) state to the Fe^{2+} (ferrous) state. [2,3]. The discharge of organic dyes, particularly MB will have a lethal impact on the environment. The investigation for novel substances with efficient photocatalytic nature has recently because of their key role in addressing environmental problems and sustainable development. Fe_3O_4 nanoparticles, renowned for their magnetic properties and catalytic potential, stand as a significant contributor in various scientific area, including catalysis, biomedicine, and environmental remediation [4,5]. Concurrently, Metal–Organic Frameworks (MOFs) are porous materials made of metal ions and organic linkers, valued for their tunable structure, high surface area, and wide applications in gas storage, separation, photocatalysis, biomedicine, sensing, drug delivery and supercapacitor [6-12] Nanoscale catalysts are extensively utilized in photodegradation processes due to their distinctive physicochemical properties and exceptionally high surface-to-volume ratio [13]. In heterogeneous photocatalysis, light absorption by a semiconductor promoting electrons to the conduction band and generating corresponding holes in the valence band and forming electron–hole (e^-/h^+) pairs. Electron–hole pairs serve as the fundamental initiators of the photocatalytic reaction. The photogenerated electrons

***To whom all correspondence should be addressed.**

reduce molecular oxygen (O_2) to form superoxide radicals ($\bullet O_2^-$) and holes oxidize water, forming reactive hydroxyl radicals (•OH). These radicals are highly reactive to decompose organic compounds to simple environmentally friendly compounds [14]. Zr and Cu-based MOFs have potential photocatalytic characteristics [15-19]. The incorporation of metal oxide nanoparticles with metal-organic frameworks (MOFs) results in increasing the band gap of the composite which improves photocatalytic activity by facilitating efficient charge separation, preventing the recombination of electron-hole pairs generated during light absorption. Band gap optimization in these composites plays a significant role in enhancing the efficiency of desired photocatalytic processes [20,21].

The integration of Fe_3O_4 nanoparticles with Zr-MOFs and Cu-MOFs into composite materials offers a synergistic approach to enhance photocatalytic activity [22]. The magnetic properties of Fe_3O_4 can facilitate easy separation and recovery of the catalyst, while the MOFs provide a high surface area and a robust framework for improved light absorption and charge carrier mobility [23]. By combining these materials, it is possible to develop composite which could be a potential photocatalysts with superior performance compared to their individual components.

The composites hold the promise of enhanced photocatalytic efficiency, owing to the amalgamation of magnetic, catalytic, and structural properties. The primary focus lies in the evaluation of photocatalytic activity, particularly in the degradation of methylene blue (MB) under sunlight irradiation. By elucidating the efficiencies of Fe_3O_4 nanoparticles, Zr-MOF, Cu-MOF, and their respective composites, this investigation aims to highlight the potential of these materials in addressing environmental pollutants, paving the way for applications in industrial pollution mitigation and sustainable environmental practices. Here in, investigation of enhanced photocatalytic performance of Fe_3O_4/Zr-MOF and Fe_3O_4/Cu-MOF composites, attributing their efficiency to optimize band gap tuning and reactive radical formation. These findings advocate their potential use in promoting environmental sustainability and addressing challenges related to mitigation of industrial pollution for green environment.

Chemicals

The chemicals, $FeSO_4 \cdot 7H_2O$, and NH_4OH were purchased from Sigma Aldrich. Cu-MOF and Zr-MOF were used as precursors. Methylene Blue (MB) (82%) which was used as a model pollutant, was bought from PT. Smart Lab, Indonesia. Each of the chemicals used during this experiment was analytically pure, and it was used just as it was received, requiring no additional purification. Additionally, deionized water (DI H_2O) was used in the stock solutions.

Methods

The FTIR spectrum was observed using KBr pellets ranging from 400 to 4000 cm^{-1} by IRPrestige-21 instrument by Shimadzu Corporation. Thermal Gravimetric analysis was performed employing a heating rate of 10 °C/s in the temperature range from 25 to 1200 °C using the TGA-50H instrument of Shimadzu Corporation. The Scanning Electron Microscopy (SEM) for morphology was measured by the EVO18 instrument manufactured by Carl Zeiss AG, UK. Elemental analysis and characterization of composition were carried out employing Energy-dispersive X-ray Spectroscopy (EDS) by the EDAX Team, USA.

Oxide Nanoparticles (Fe_3O_4 NPs) Synthesis

The 25 mL of water was needed to dissolve 0.5 g of $FeSO_4 \cdot 7H_2O$. The ammonium hydroxide (3.75 mL) was added to this solution with stirring. The resultant suspension was allowed for continuous stirring for 10 min for oxidation of iron (II). The reaction mixture was then transferred to a sealed pressure vessel and autoclaved with a volume of 100 mL at 130 °C for 4 h then allowed for cooled down to room temperature (Fig 1). The black precipitate was filtered off and purified with water as a dispersant followed by centrifugation. Lyophilization of the final Fe_3O_4 NPs suspension resulted in a black dry powder. The product is dried and collected.

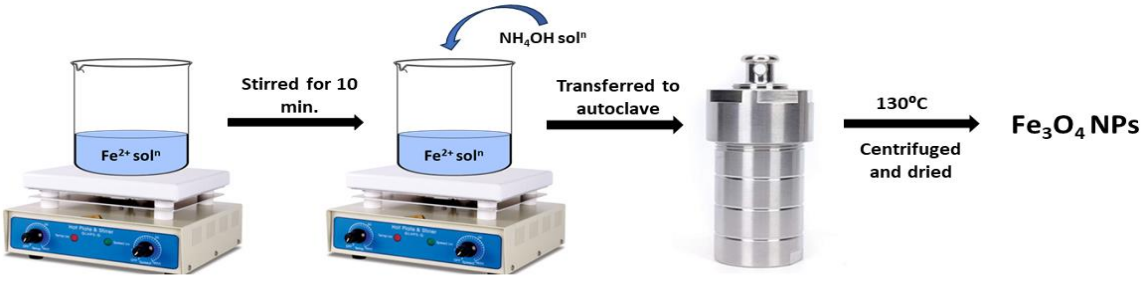

Fig. 1: Schematic diagram of Fe_3O_4 nanoparticles synthesis by hydrothermal.

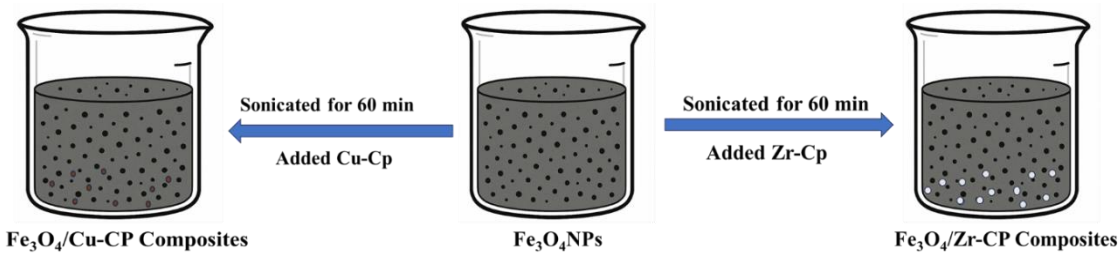

Fig. 2: Schematic diagram of synthesis of Fe_3O_4/Zr-CP and Fe_3O_4/Cu-CP composites by sonication.

Fe_3O_4/Zr-MOF and Fe_3O_4/Cu-MOF composite synthesis

A 25 mL of 85% Fe_3O_4 colloidal suspension was prepared in a 100 mL beaker. Then 25 mL of 15% Cu-MOF and Zr-MOF colloidal suspension was added to Fe_3O_4 suspension (Fig 2). The resultant suspension was sonicated for 60 minutes. The product was repeatedly washed and centrifuged with water and the brown Fe_3O_4/Cu-MOF and Fe_3O_4/Zr-MOF composite was recovered. Then the product was dried under vacuum pump and kept in desiccator.

Photodegradation of methylene blue (MB)

The 5-ppm methylene blue solution was prepared by deionized water and 100 mL methylene blue solution was taken into a beaker and pH 9.2 was maintained. The 0.1 g/L of Fe_3O_4 nanoparticles, Fe_3O_4/Zr-MOF and Fe_3O_4/Cu-MOF composite as photocatalysts was added with stirring to the same, 5 ppm MB solution. The resultant mixture of MB solution and catalyst exposed to sun light and the sample was collected periodically at constant interval of time (0, 30, 60, 90 and 120 minutes) into the falcon tube. The degradation was measured by measuring concentration of methylene blue using a UV-Vis spectrometer over certain period. The absorption spectra were recorded to monitor the degradation of methylene blue over time. Finally, the percentage of degradation of methylene blue was calculated using the initial and final concentrations obtained from the absorption spectral data. The degradation percentage was resolved applying the following equation [24].

$$\text{Degradation Efficiency (\%)} = \frac{C_o - C}{C_o} \times 100$$

Result and Discussions

FTIR

The chemical structure of Zr-CP, Fe_3O_4 NPs, and Fe_3O_4/Zr-CP composite is studied by FTIR spectroscopy (Fig 3). The dispersion of Fe_3O_4 nanoparticles in the polymer matrix has been confirmed through FTIR spectrum analysis.

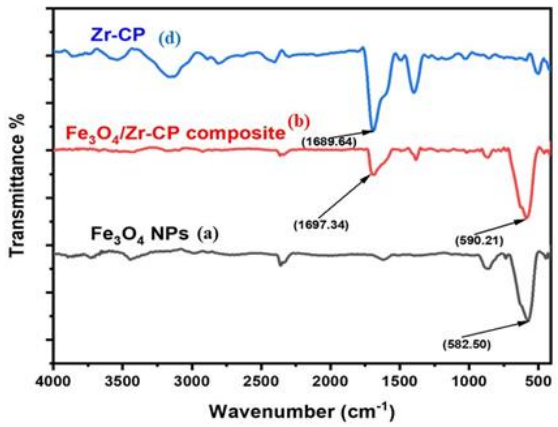

Fig. 3: FTIR spectra of Zr-CP (d), Fe_3O_4/Zr-CP (b) composite and Fe_3O_4 NPs (a).

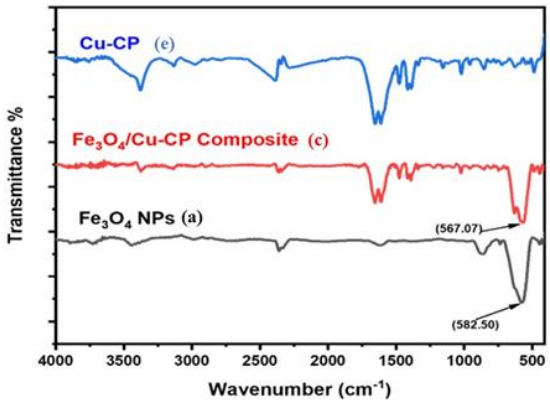

Fig. 4: FTIR spectra of Cu-CP (e), Fe_3O_4/Cu-CP (c) composite and Fe_3O_4 NPs (a).

The band at 582.50 cm^{-1} of IR spectra of Fe_3O_4 NPs (Fig 3) is attributed for Fe–O bond indicates nanoparticles of Fe_3O_4. The peaks at 580 cm^{-}

^{1} and 1689.64 cm^{-1} in the spectra of Zr-CP is attributed for Cu–O and C=O bonds respectively, indicates the coordination polymer. The peaks at 590.21 cm^{-1} and 1697 cm^{-1} in the spectra of Fe_3O_4 /Zr-CP composite is attributed for the vibrations of Cu–O and C=O bonds shifted than coordination polymer, which indicates the formation of coordination polymer.

The IR spectra of Fe_3O_4 NPs (Fig 4) vibration of Fe–O is observed at 582.50 cm^{-1}. The peak at 567.07 cm^{-1} of Fe_3O_4 /Cu-CP composite spectra is assigned for the vibrations of Fe–O (Fig 4). The shifting of the peak of Fe–O at 582.50 cm^{-1} to 567.07 cm^{-1} has indicates the composite formations.

TGA

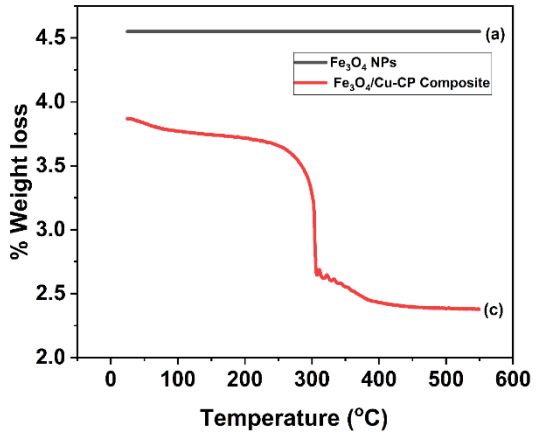

Fig 5: TGA pattern of Fe_3O_4 NPs (a) and Fe_3O_4/Cu-CP Composite (c).

The thermo-gravimetric analysis of synthesized materials Fe_3O_4 NPs and Fe_3O_4/Cu-CP composites represent the thermal stability. The thermo-gravimetric graph indicates (Fig 5) the Fe_2O_3 NPs is the most stable at the temperature range 0 °C to 550 °C. The graph of Fe_3O_4/Cu-CP Composites was decreased very slowly up to 280 °C that indicate the weight loss for H_2O removing and other weak bonding, from this temperature up to 300 °C sharply lost the weight which actually indicate the all-coordination bond of CP is sharply broken. The weight loss from 300 °C to 550 °C because of breaking of other bonding, particularly bonding of metal with oxide.

The weight loss is less steep in this region from 450 °C to 550 °C is attributed for strong bond of metal with oxide. Finally, it is observed that nanoparticles are thermally more stable than composite.

Cyclic Voltammetry

Cyclic Voltammetry (CV) is an electrochemical technique applied to study the electrochemical behavior of a material or a redox reaction. It is widely utilized in various fields, including analytical chemistry, materials science, and electrochemical research. The technique involves applying a controlled potential voltage to an electrochemical cell and measuring the resulting current while the potential is varied in a cyclical manner. This process provides valuable information about the oxidation and reduction occurring within the sample. The CV curves (Fig 6) depict the Cu-CP and Fe_3O_4/Cu-CP composite redox couple using a GC (Glassy carbon) electrode with various scan rates between -1.5 and 0.2 V (vs. Ag/AgCl) at room temperature. Cyclic voltammetry (CV) curves of Cu-CP in 0.1 M KCl electrolyte were collected using a GC working electrode at various scan rates to define the potential region for redox reactions (Fig 6(a)), in which the potential window for Cu^{+}/Cu^{0} and Cu^{2+}/Cu^{+} was over -0.8 V. The significant drop in current is characteristic of a nucleation loop, indicating the deposition of Cu metal onto the GC electrode. On the other hand, in composite (Fig 6(b)) the well-known reduction peak of Fe^{+2} is observed, which is irreversibly reduced near -1.2 V. The composite's formation is confirmed by CV to the current peak of Cu and Fe present in (Fig 6(b))

UV-Vis

The very significant properties of the materials such as electronic transition and band gap was found from the UV-Vis spectra. The UV–Vis absorption spectra of Fe_3O_4 NPs, Cu-CP and Fe_3O_4/Cu-CP composite are presented (Fig 7). The broad peak at 258 nm in the Cu-CP spectra is attributed for n→π* transition due to presence of lone pair in N and O.

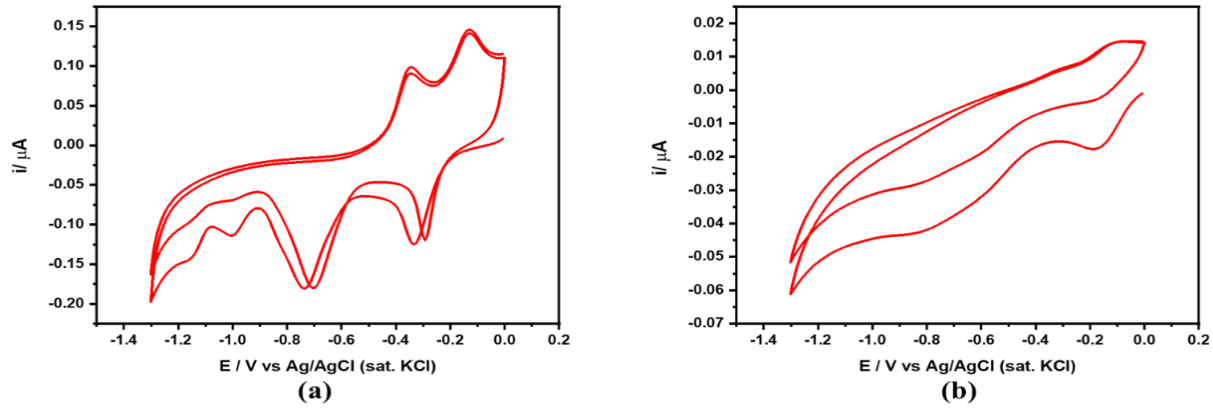

Fig. 6: CV curves of (a) Cu- CP and (b) Fe_3O_4/Cu-CP composite in a 0.1 M KCl using GC electrode at various scan rates.

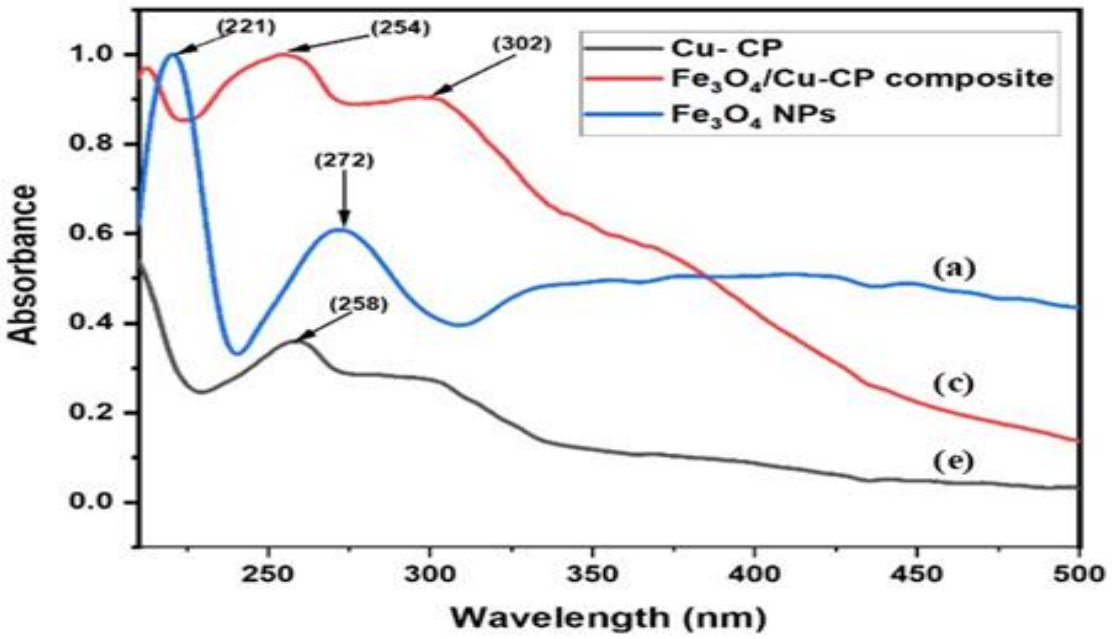

Fig. 7: UV- Vis spectra of Fe_3O_4 NPs (a), Fe_3O_4/Cu-CP composite (c) and Cu-CP (e).

The sharp peaks at the 221 nm and 272 nm in the spectra is attributed for d→d and d→p transition. The broad band in the region of 254 nm and 302 nm of the Fe_3O_4/Cu-CP composite spectra is attributed for π→π* and n→π* transition [25]. The presence and shifting of the peak indicate formation composite.

Band gap analysis

The calculation of band gap values is carried out using the equation $\alpha=A(h\nu-Eg)^n/h\nu$ where α, E_g and A are the absorption coefficient, band gap and constant respectively. The band gap plays a key role for being an efficient photocatalyst, the band gap of a standard photocatalyst TiO_2 is approximately 3.2 eV [26]. It indicates that band gap in the range of 2.0 eV to 4.0 eV could be a potential photocatalyst. The band gap of Fe_3O_4 (NPs) and Fe_3O_4/Cu-MOF composite is 1.95 eV and 2.54 eV respectively (Fig 8), whereas the band gap for TiO_2 is approximately 3.2 eV which is established photo-catalyst.

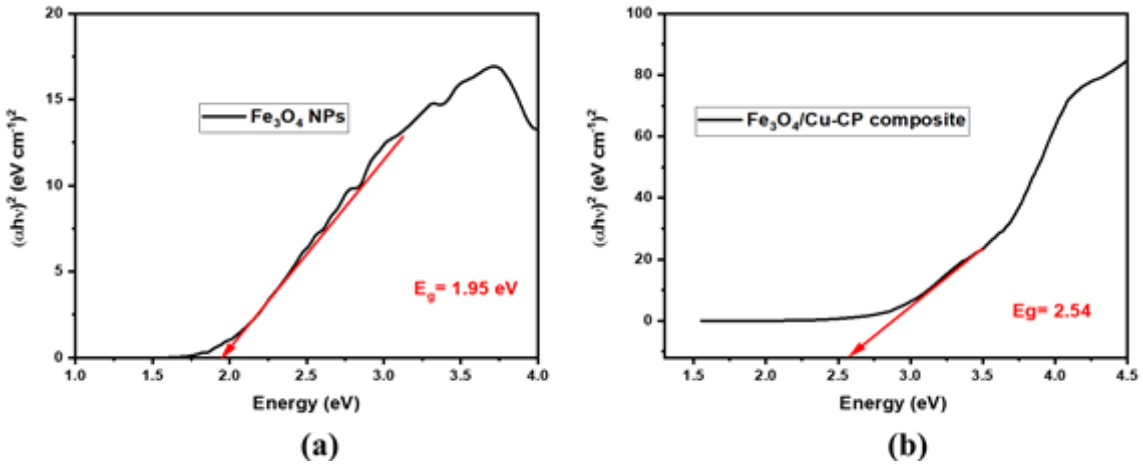

Fig. 8: Tauc plot for band gap calculation of (a) Fe_3O_4 NPs and (b) Fe_3O_4/Cu-CP composite.

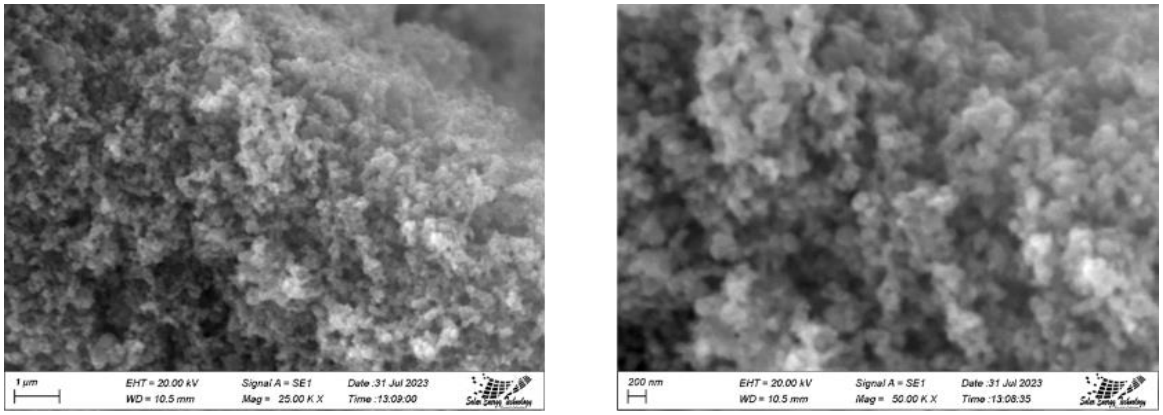

Fig. 9: SEM image of (a) Fe_3O_4/Zr-CP composite 25.00 KX and (b) Fe_3O_4/Zr-CP composite 50.00 KX

So, the synthesized nanoparticles and composite could be a potential photocatalyst. Integrating Fe3O4 NPs into Zr-MOF and Cu-MOF tunes the bandgap and optimizing radical generation, which boosts the degradation of MB dye.

Scanning electron microscopy (SEM)

A Scanning Electron Microscope (SEM) is a sophisticated scientific instrument that uses a focused beam of electrons to create detailed images and gather information about the surface of diverse materials. It provides high-resolution images and valuable insights into the microstructure, topography, composition, and other surface properties of samples. Analyzing SEM images is a pivotal stage within the comprehensive characterization process, particularly in the realm of topographic investigations involving samples.

The SEM images in (Fig 9(a)) show the porous and fluffier structure of Fe_3O_4/Zr-CP composite. The captured image in (Fig 9(b)) is at the length of 100 nm. So, it can be said that the size of the Fe_3O_4/Zr-CP composite within the nanometer range (Fig 10(a-b)). The morphology of the composite mostly appeared to be porous and spongy.

EDS

To verify the successful formation of the Fe_3O_4/Zr-CP composite EDX analysis was performed. During the EDX measurement different areas were analyzed and the corresponding peaks are shown in (Fig 11).

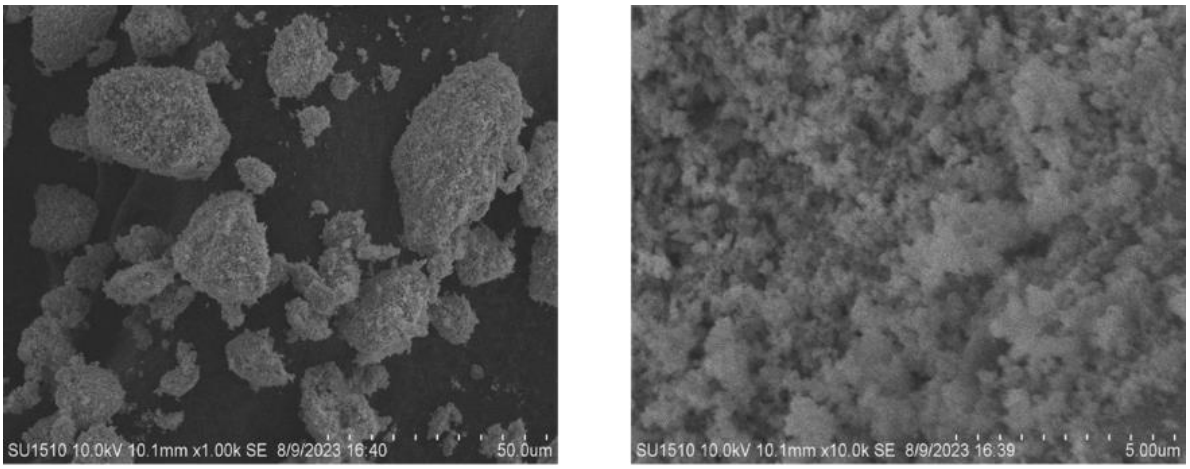

Fig.10: SEM image of (a) Fe_3O_4/Cu-CP composite 1.00 KX and (b) Fe_3O_4/Cu-CP 10.00 KX composite.

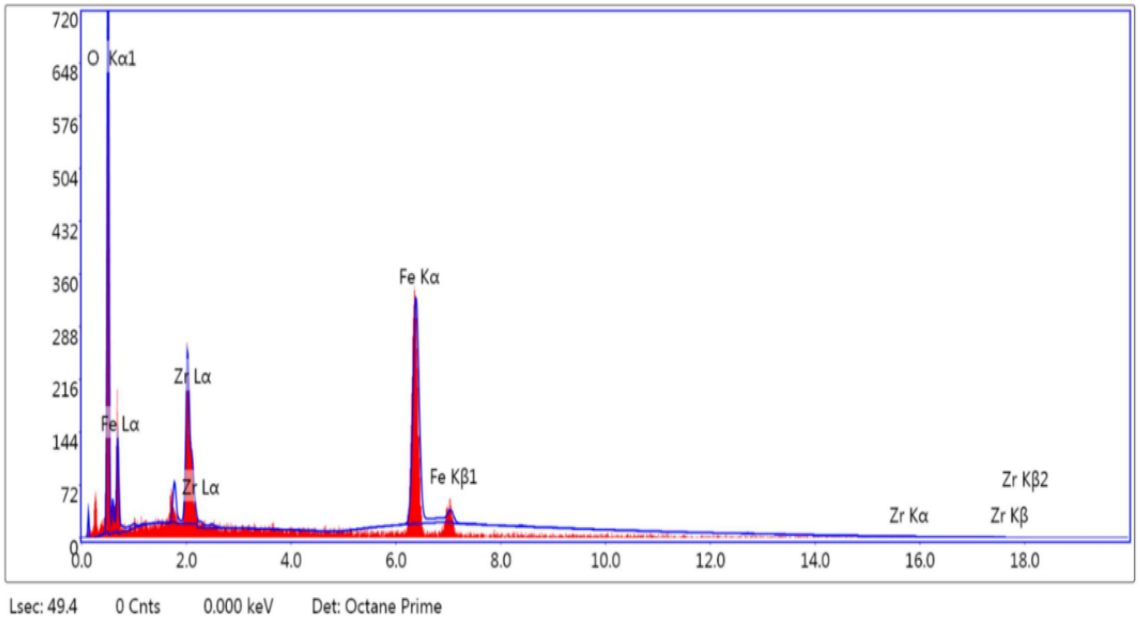

Fig. 11: EDS spectra of Fe_3O_4/Zr-CP composite.

The EDS spectrum of the synthesized composite evidently shows the presence of both Fe_3O_4 nanoparticles and Zr-CP components. In spectrum, the quantity of O, Zr, and Fe are 38.31, 15.43, and 46.26 weight % respectively that indicates the formation of composite. Details of the EDS spectra of this composite atomic and weight % are listed in (Table 1).

Photocatalytic activity

The photocatalytic performance of Fe_3O_4 NPs, Fe_3O_4/Zr-CP composite and Fe_3O_4/Cu-CP composite to degrade MB is illustrated by the peaks produced by a UV-vis spectrometer and shown in (Fig 12 (a-c)).

Table-1: EDS weight ratio of Fe_3O_4/Zr-CP composite.

Element	Weight %	Atomic %
Oxygen (O)	38.41	70.60
Zirconium (Zr)	15.43	4.99
Iron (Fe)	46.26	24.42

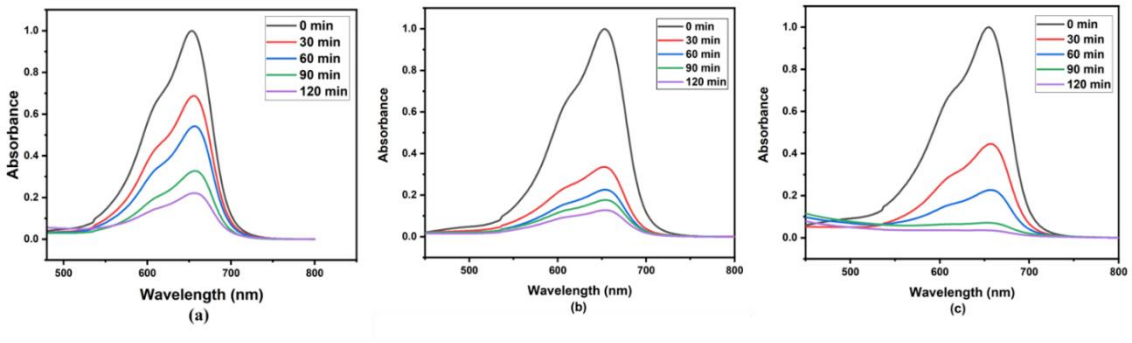

Fig. 12: The degradation of MB by (a) Fe_3O_4 NPs, (b) Fe_3O_4/Zr-CP composite and (c) Fe_3O_4/Cu-CP composite.

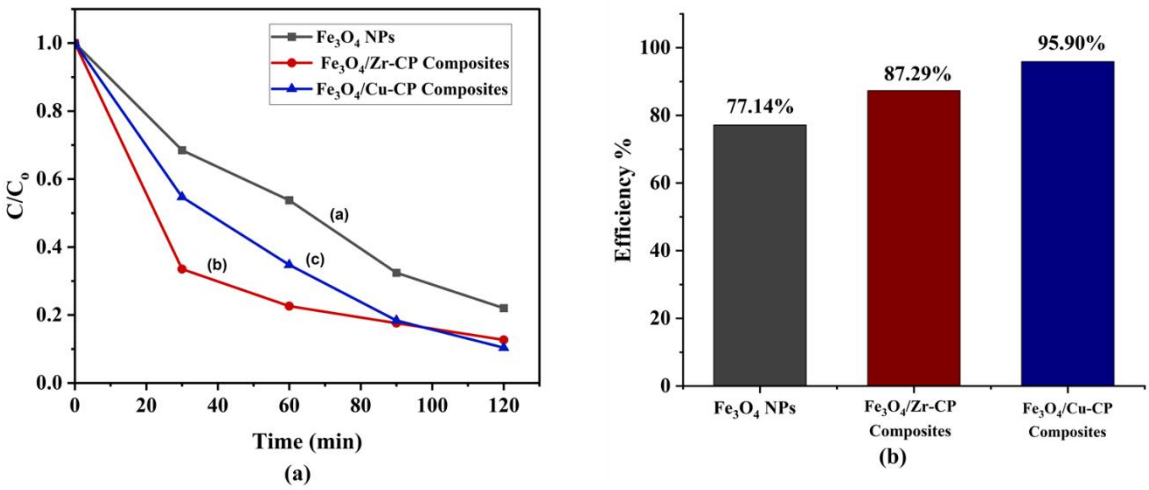

Fig 13: (a) The decreasing manner of C/C_o and (b) efficiency after 120 min of MB degradation by Fe_3O_4 NPs (a), Fe_3O_4 /Zr-CP composite (b) and Fe_3O_4 /Cu-CP composite (c).

The same cuvette is used for each measurement. The beer-Lambert equation states that the concentration is directly proportional to the absorption. There was a decrease in absorbance observed. The ratio of concentration at any time (C) with initial concentration (C_o) (C/C_o) was decreased over time when Fe_3O_4 NPs, Fe_3O_4 /Zr-CP composite and Fe_3O_4 /Cu-CP composite was used as photocatalyst for MB degradation (Fig 13(a)).

The degradation was monitored for 120 minutes in the sun irradiation, the degradation of methylene blue (MB) was 77.14% in the presence of Fe_3O_4 NPs as a photocatalyst. Whereas, in the presence of Fe_3O_4 /Zr-CP and Fe_3O_4/Zr-CP composite as photocatalysts, shown the degradation efficiency of MB of 87.29% and 95.90%, respectively. (Fig 13(b)). It is clear that composite showed the significantly higher activity than nanoparticles. So, it was revealed that incorporation of Fe_3O_4 NPs to CP for preparing Fe_3O_4 /Zr-CP composite increase the degradation efficiency by tuning the band gap to optimum level. There is a strong correlation of band gap and photo degradation efficiency. It was found that the composite band gap is higher than nanoparticle and closer to TiO_2. The composite can form (e/h) and retain required time to initiate photodegradation. So, this composite is potential photocatalyst to degrade the dye and could be used for various industrial and environmental purposes.

Kinetic of Photodegradation

Photodegradation reactions commonly described by first-order kinetics, where the degradation rate is directly proportional to the dye concentration. The kinetic of degradation was observed for Fe_3O_4 NPs, Fe_3O_4/Zr-CP composites and Fe_3O_4/Cu-CP composites. The kinetic of MB dye degradation in the presence of Fe_3O_4 NPs, Fe_3O_4/Zr-CP composites and Fe_3O_4/Cu-CP composites (Fig 14) show a plot of $-\ln(C/C_0)$ verses time to comprehend the reaction rate constant and obtained straight lines. The Fe_3O_4 NPs, Fe_3O_4/Zr-CP composites, Fe_3O_4/Cu-CP

composites respective regression value (R^2) is found to be 0.98384, 0.99294 and 0.99588.

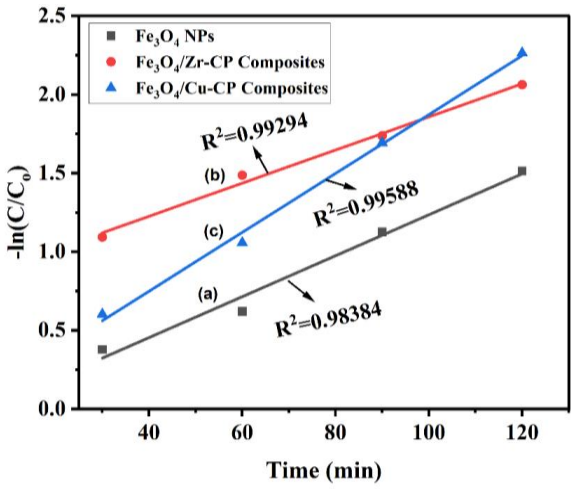

Fig. 14: Pseudo-first-order kinetics plots of MB adsorption on with Fe_3O_4 NPs (a), Fe_3O_4/Zr-CP (b) composites and Fe_3O_4/Cu-CP composites (c).

The experimental data indicate that the photocatalytic degradation of methylene blue follows first-order reaction mechanism as the regression values for the fitted lines to be $R^2 > 0.95$ [27]. The calculated rate constant, k (min^{-1}) of Fe_3O_4 NPs, Fe_3O_4/Zr-CP composites, Fe_3O_4/Cu-CP composites are 1.303×10^{-2} min^{-1}, 1.053×10^{-2} min^{-1} and 1.873×10^{-2} min^{-1} respectively. Such kinetic behavior has been widely reported in similar photocatalytic studies, and confirms the efficiency of the photocatalyst in promoting dye decomposition through a first-order pathway [28].

Conclusion

Finally, it can be said that our proposed nanoparticle, Fe_3O_4 and the composites, Fe_3O_4/Zr-CP and Fe_3O_4/Cu-CP have been synthesized successfully. The provided characterization data UV-Vis spectroscopy, FTIR spectroscopy, TGA, SEM and EDX have affirm the formation of the desired products. After that the photocatalytic activities of the synthesized products have been studied and the study showed that our synthesized composites are better photocatalysts than the Fe_3O_4 NPs. Hence, these composites can have effective implementations in sectors, notably in the industrial waste water treatment plants in our country. The composites have been proved as stable and efficient catalysts; thus, these might be further applied in photosensitizers, energy storage etc. in future.

Acknowledgment

The authors wish to thank Shahjalal University of Science and Technology, Research Center for the Promotional Research Grant (Project ID: PS/2024/1/02, 2024-2025).

References

1. M. Zahid-Hussain, A. Schneemann, R.A. Fischer, Y. Zhu, and Y. Xia, MOF derived porous ZnO/C nanocomposites for efficient dye photodegradation, ACS Appl. *Energy Mater*., **1**, 4695 (2018).
2. A. Norouzi, and A. Nezamzadeh-Ejhieh, Investigation of the simultaneous interactions of experimental variables and mechanism pathway in the photodegradation of methylene blue by binary ZnO/Cu_2O photocatalyst, *Materials Res. Bul.*, **164**, 112237 (2023).
3. S. A. Mirsalari, A. Nezamzadeh-Ejhieh, and A. R. Massah, A Z-scheme CdS/Ag_3PO_4 catalyst: Characterization, experimental design and mechanism consideration for methylene blue, *Spectrochi. Acta Part A: Mol. and Biomo. Spect.*, **288**, 122139 (2023).
4. B. Rezaei, P. Yari, S. M. Sanders, H. Wang, V. K. Chugh, S. Liang, and K. Wu, Magnetic nanoparticles: a review on synthesis, characterization, functionalization, and biomedical applications, Small, **20(5)**, 2304848 (2023).
5. M. T. Yaraki, S. Zahed Nasab, I. Zare, M. Dahri, M. Moein Sadeghi, M. Koohi, and Y. N. Tan, Biomimetic metallic nanostructures for biomedical applications, catalysis, and beyond, *Indus. & Eng. Chem. Res.*, **61(22)**, 7547-7593 (2022).
6. G. Cai, P. Yan, L. Zhang, H. C. Zhou, and H. L. Jiang, Metal–organic framework-based hierarchically porous materials: synthesis and applications, *Chem. Rev.*, **121(20**), 12278 (2021).
7. L. Jiao, J. Y. R. Seow, W. S. Skinner, Z. U. Wang, and H. L. Jiang, Metal–organic frameworks: Structures and functional applications, *Mat. Today*, **27**, 43-68 (2019).
8. Y. S. Wei, M. Zhang, R. Zou, and Q. Xu, Metal–organic framework-based catalysts with single metal sites, *Chem. Rev.*, **120(21)**, 12089 (2020).
9. P. Horcajada, T. Chalati, C. Serre, B. Gillet, C. Sebrie, T. Baati, and R. Gref, Porous metal–organic-framework nanoscale carriers as a potential platform for drug delivery and imaging, *Nature Mat.*, **9(2)**, 172 (2010).
10. B. Chen, L. Wang, F. Zapata, G. Qian, and E. B. Lobkovsky, A luminescent microporous metal–

organic framework for the recognition and sensing of anions, *J. of the Ame. Chem. Soc.*, **130(21)**, 6718 (2008).
11. A. J. Fletcher, K. M. Thomas, and M. J. Rosseinsky, Flexibility in metal-organic framework materials: Impact on sorption properties, *J. of S. State Chem.*, **178(8)**, 2491 (2005).
12. H. Yao, F. Zhang, G. Zhang, H. Luo, L. Liu, M. Shen, and Y. Yang, A novel two-dimensional coordination polymer-polypyrrole hybrid material as a high-performance electrode for flexible supercapacitor, *Chem. Eng. J.*, **334**, 2547 (2018).
13. D. Ayodhya, and G. Veerabhadram, A review on recent advances in photodegradation of dyes using doped and heterojunction-based semiconductor metal sulfide nanostructures for environmental protection, *Mat. Today Ener.*, **9**, 83 (2018).
14. A. Noruozi, and A. Nezamzadeh-Ejhieh, Preparation, characterization, and investigation of the catalytic property of α-Fe_2O_3-ZnO nanoparticles in the photodegradation and mineralization of methylene blue, *Chem. Phy. L.*, **752**, 137587 (2020).
15. J. Li, J. Y. Huang, Y. X. Meng, L. Li, L. L. Zhang, and H. L. Jiang, Zr-and Ti-based metal–organic frameworks: synthesis, structures and catalytic applications, *Chem. Comm.*, **59(18)**, 2541 (2023).
16. Y. C. Lopez, H. Viltres, N. K. Gupta, P. Acevedo-Pena, C. Leyva, Y. Ghaffari, and K.S. Kim, Transition metal-based metal–organic frameworks for environmental applications: a review, *Env. Chem. L.*, **19**, 1295 (2021).
17. D. Y. Lee, D. V. Shinde, S. J. Yoon, K. N. Cho, W. Lee, N. K. Shrestha, and S. H. Han, Cu-based metal–organic frameworks for photovoltaic application, *The J. of Physical Chem. C*, **118(30)**, 16328 (2014).
18. M. B. Gawande, A. Goswami, F. X. Felpin, T. Asefa, X. Huang, R. Silva, and R. S. Varma, Cu and Cu-based nanoparticles: synthesis and applications in catalysis, *Chem. Rev.* **116(6)**, 3722 (2016).
19. M. M. Alam, M. F. Ahmed, M. A. Arafath, M. R. Karim, M. N. Uddin, and M. S. Hossain, (2024). Synthesis of Cu and Zr-based coordination polymers with N/O donors and investigation of their photocatalytic activity against dye, *Heliyon*, **10(12)** (2024).
20. J. Guo, Y. Liang, L. Liu, J. Hu, H. Wang, W. An, and W. Cui, Noble-metal-free CdS/Ni-MOF composites with highly efficient charge separation for photocatalytic H_2 evolution, *App. Surf. Sci.*, **522**, 146356 (2020).
21. S. Subudhi, S. P. Tripathy, and K. Parida, Metal oxide integrated metal organic frameworks (MO@ MOF): rational design, fabrication strategy, characterization and emerging photocatalytic applications, *Inorganic Chem. Fron.*, **8(6)**, 1619 (2021).
22. Y. Bai, C. Liu, Y. Shan, T. Chen, Y. Zhao, C. Yu, and H. Pang, Metal-organic frameworks nanocomposites with different dimensionalities for energy conversion and storage, *Adv. Ener. Mat.*, **12(4)**, 2100346 (2022).
23. L. Chen, J. Peng, F. Wang, D. Liu, W. Ma, J. Zhang, and H. He, ZnO nanorods/Fe_3O_4-graphene oxide/metal-organic framework nanocomposite: recyclable and robust photocatalyst for degradation of pharmaceutical pollutants, *Env. Sci. and Poll. Res.*, **28**, 21799 (2021).
24. R. H. Riyan, M. H. Arafath, S. S. Alam, and M. O. Faruk, AG_2O Nanoparticle and Its Composite with Coordination Polymers of Cu: Synthesis, Characterisation and Photocatalytic Activity, *Platform: A J. of Sci. and Tech.*, **6(2)**, 17 (2023).
25. Z. I. Takai, M. K. Mustafa, S. Asman, and K. A. Sekak, Preparation and characterization of magnetite (Fe_3O_4) nanoparticles by sol-gel method, *Int. J. Nanoelectron. Mater*, **12(1)**, 37 (2019).
26. M. I. Dar, A. K. Chandiran, M. Grätzel, M. K. Nazeeruddin, and S. A. Shivashankar, Controlled synthesis of TiO_2 nanoparticles and nanospheres using a microwave assisted approach for their application in dye-sensitized solar cells, *J. of Mat. Chem. A*, **2(6)**, 1662 (2014).
27. S. Alkaykh, A. Mbarek, and E. E. Ali-Shattle, Photocatalytic degradation of methylene blue dye in aqueous solution by $MnTiO_3$ nanoparticles under sunlight irradiation., *Heliyon*, **6(4)** (2020).
28. A. NezamSzadeh-Ejhieh, and Z. Banan, Kinetic investigation of photocatalytic degradation of dimethyldisulfide by zeolite A containing nano CdS, *Iran. J. of Cat.*, **2(2)** (2012).